

# Neutron Diffraction Studies of $\text{Pr}_2\text{C}_3$ , $\text{Nd}_2\text{C}_3$ , and $\text{Dy}_2\text{C}_3$ at 300 to 1.6°K\*

MASAO ATOJI

*Chemistry Division, Argonne National Laboratory, Argonne, Illinois 60439*

Received December 19, 1977; in revised form March 9, 1978

Neutron diffraction measurements have shown that the body-centered cubic  $\text{Pr}_2\text{C}_3$ ,  $\text{Nd}_2\text{C}_3$ , and  $\text{Dy}_2\text{C}_3$  become antiferromagnetic below 8, 24, and 22°K, respectively, all exhibiting the  $\text{Tb}_2\text{C}_3$ -type magnetic structure. In the uniaxial moment model having two antiferromagnetic and two paramagnetic body diagonals, the saturation order moments per metal atom are 1.3, 3.0, and 9.5 Bohr magnetons, respectively, being 41, 92, and 95% of the respective free ion values.  $\text{Pr}_2\text{C}_3$  shows an exceptionally large crystal field effect. The antiferromagnetic alignment is uninfluenced by the applied field of up to 21 kOe. The crystal structure data at 300 to 1.6°K are also given. A brief review is presented on the physical properties of the rare earth sesquicarbides.

## Introduction

The rare earth sesquicarbides,  $(\text{RE})_2\text{C}_3$ , exhibit two different structure types,  $\alpha$  and  $\delta$ .  $\alpha$ - $(\text{RE})_2\text{C}_3$  is isostructural with the body-centered cubic  $\text{Pu}_2\text{C}_3$  ( $D5_c$ ) and stable for RE = La-Ho (Pm and Eu have not been examined) (1,2).  $\delta$ - $(\text{RE})_2\text{C}_3$  exists for RE = Ho (dimorphic), Er, Tm, Lu, and Y (1,3). The crystal structure of  $\delta$ - $(\text{RE})_2\text{C}_3$  has not been determined since only the powder diffraction data are available, indicating an unsolvably complex, noncubic structure (3). High-pressure synthesis can stabilize the  $\alpha$ - $(\text{RE})_2\text{C}_3$  structure for RE = Er, Tm, Yb, and Y (4). Upon annealing, the high-pressure structure reverts to the ambient-pressure phase. Some of the  $\text{Pu}_2\text{C}_3$ -type carbides possess high superconducting transition temperatures  $T_0$ . The highest known  $T_0$  in the binary system is 11°K

\* Work performed under the auspices of the Division of Basic Energy Sciences of the Department of Energy. The publisher acknowledges the U.S. Government's right to retain a nonexclusive royalty-free license in and to any copyright covering this paper for government purposes.

of  $\text{La}_2\text{C}_3$  (5,6), and that in the ternary system is 17°K of  $\text{Y}_{1.4}\text{Th}_{0.6}\text{C}_{3.1}$  (7). Only two other structure types,  $\text{W}_3\text{O}$  (A15) and  $\text{NaCl}$  (B1), are known to have  $T_0$  above 15°K. The present study is to provide further insight into the electronic and bond structures of  $\alpha$ - $(\text{RE})_2\text{C}_3$ . Throughout this paper, when no specification is made as to  $\alpha$  or  $\delta$ , we refer to the  $\alpha$  structure.

Neutron diffraction studies have been carried out at 296°K for  $\text{La}_2\text{C}_3$  and  $\text{Pr}_2\text{C}_3$  (8), and at 296 to 5°K for  $\text{Ce}_2\text{C}_3$  (9),  $\text{Tb}_2\text{C}_3$  (10), and  $\text{Ho}_2\text{C}_3$  (11). Neutron magnetic scattering has shown that the rare earth atom in the paramagnetic  $(\text{RE})_2\text{C}_3$  is of tripositive Hund ground state, except for  $\text{Ce}_2\text{C}_3$ , in which Ce changes gradually from +3.4 to +4 on cooling from 296 to 80°K.  $\text{Tb}_2\text{C}_3$  and  $\text{Ho}_2\text{C}_3$  become antiferromagnetic below 33 and 19°K, respectively, displaying entirely different moment alignments. The neutron studies of  $\text{Pr}_2\text{C}_3$ ,  $\text{Nd}_2\text{C}_3$ , and  $\text{Dy}_2\text{C}_3$  at 296 to 1.6°K reported here signify completion of the neutron structure survey of the accessible  $(\text{RE})_2\text{C}_3$ , excluding  $\text{Sm}_2\text{C}_3$  and  $\text{Gd}_2\text{C}_3$  which have pro-

hibitively high neutron attenuation. Regarding the experimental uncertainty, the standard deviation in the last significant digit is given in parentheses.

### Preparatory Data

The samples were prepared by arc-melting compressed pellets of a stoichiometric mixture of rare earth metal filing (99.9% pure) and spectroscopic grade graphite powder. Brassy metallic  $(RE)_2C_3$  buttons were then pulverized to 200-mesh powder and their diffraction data were taken using a multipurpose diffractometer (12) set for the neutron wavelength  $\lambda = 1.069 \text{ \AA}$  (0.0716 eV). The total cross section of Dy for thermal neutrons is exceptionally large (630 barns at 0.0716 eV). Hence,  $Dy_2C_3$  was intermixed with aluminum powder (15 barns) so as to increase the scattering-to-attenuation ratio. The optimum mixing ratio chosen was  $Dy_2C_3:Al = 1:1.1$  by weight for a packing density of  $1.7 \text{ g/cm}^3$  in a cylindrical holder of 1 cm diameter.  $(RE)_2C_3$  melts incongruently (3, 13) and hence second-phase contamination is inevitable in the routine

synthesis. All our samples contain up to several weight percent of the respective dicarbides. The neutron data of  $PrC_2$  (14),  $NdC_2$  (14), and  $DyC_2$  (15) at 296 to 4°K are available and hence the impurity intensity subtraction could readily be made using the differential pattern technique. The diffraction patterns of  $Pr_2C_3$ ,  $Nd_2C_3$ , and  $Dy_2C_3$  at 4°K are shown in Figs. 1, 2, and 3, respectively, where the impurity reflections have been subtracted out. In these figures, subscripts to the indices, m and n, signify the magnetic and nuclear reflections. The reflection without the subscript comprises both the magnetic and nuclear intensities.

The cubic lattice constants of  $Pr_2C_3$ ,  $Nd_2C_3$ , and  $Dy_2C_3$  are, respectively,  $a = 8.590(6)$ ,  $8.534(2)$ , and  $8.206(3)$  at 296°K and  $8.572(2)$ ,  $8.517(2)$ , and  $8.189(3)$  at 4°K. The average linear thermal expansion coefficient in the range 4 to 296°K is  $6 \times 10^{-6} \text{ deg}^{-1}$  in all cases, indicating neither large magnetostriction nor unusual valence modulation, as found in  $Ce_2C_3$  (9). The positional parameters in  $T_d^6 - I43d$  (16) are RE at  $16(c)$  ( $uuu$ ) with  $u = 0.0515(4)$ ,  $0.0516(7)$ , and

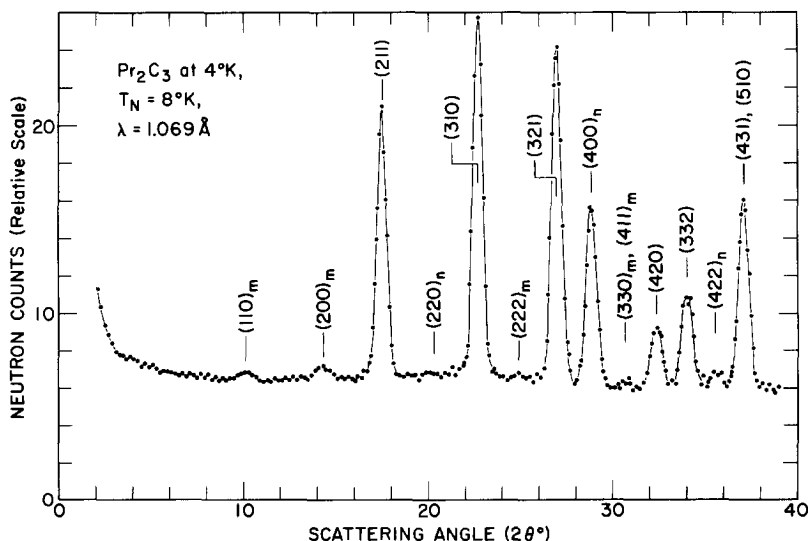


FIG. 1. Neutron diffraction pattern of the antiferromagnetically ordered  $Pr_2C_3$  at 4°K. The magnetic intensities are all very weak. Hence, the diffraction pattern of the paramagnetic  $Pr_2C_3$  is almost identical to the 4°K pattern excluding a few low-angle magnetic peaks.

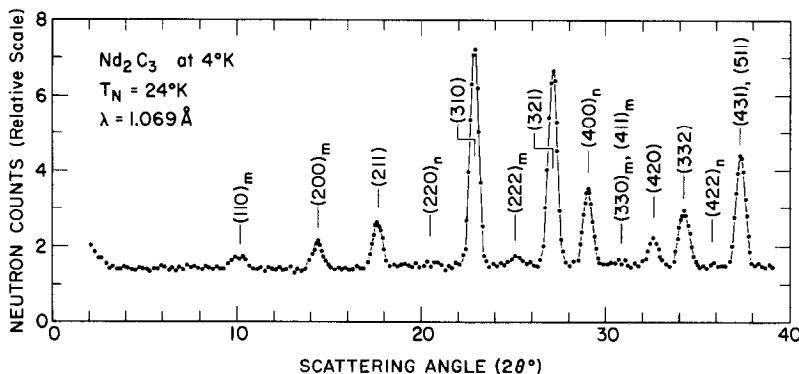


FIG. 2. Neutron diffraction pattern of the antiferromagnetically ordered  $\text{Nd}_2\text{C}_3$  at  $4^\circ\text{K}$ .

0.0514(8) and C at  $24(d)$  ( $v, 0, 1/4$ ) with  $v = 0.3029(2)$ ,  $0.3024(6)$ , and  $0.2994(8)$ . The temperature factor coefficients are  $2B = 3.3(4)$ ,  $3.2(4)$ , and  $3.0(4)$  at  $296^\circ\text{K}$  and  $0.4(1)$  for all at  $4^\circ\text{K}$ .

### Magnetic Structure

The paramagnetic scattering in  $\text{Nd}_2\text{C}_3$  and  $\text{Dy}_2\text{C}_3$  at  $296^\circ\text{K}$  gave the effective Bohr magneton numbers of  $3.6(3)$  and  $10.6(6)$ , respectively, in agreement with  $g[J(J+1)]^{1/2}$  of the trivalent Hund ground state, where  $g$  is the Landé factor and  $J$  is the total angular momentum. A similar result has previously been obtained for  $\text{Pr}_2\text{C}_3$  (8). At  $4^\circ\text{K}$ ,  $\text{Pr}_2\text{C}_3$ ,  $\text{Nd}_2\text{C}_3$ , and  $\text{Dy}_2\text{C}_3$  exhibit a set of coherent magnetic reflections which are very much

analogous to those of  $\text{Tb}_2\text{C}_3$ . The magnetic intensities of  $\text{Pr}_2\text{C}_3$  are especially weak, as exemplified by the magnetic (200) reflection which is only several percent of the nuclear (310) reflection in intensity. Hence, the experimental error of the  $\text{Pr}_2\text{C}_3$  magnetic data presented here is considerably large unless specified otherwise.

The temperature dependency of the magnetic (200) reflection leads Néel temperatures ( $T_N$ ),  $8(2)$ ,  $24(2)$ , and  $22(2)^\circ\text{K}$  for  $\text{Pr}_2\text{C}_3$ , and  $\text{Nd}_2\text{C}_3$ , and  $\text{Dy}_2\text{C}_3$ , respectively. The resulting spontaneous magnetization curves, as shown in Fig. 4, appear to follow the Brillouin function for  $J = 3$ , while the free ion  $J$  values are 4, 4.5, and 7.5 for  $\text{Pr}^{3+}$ ,  $\text{Nd}^{3+}$ , and  $\text{Dy}^{3+}$ , respectively. Despite the difference in the magnetic structure, the magnetization in

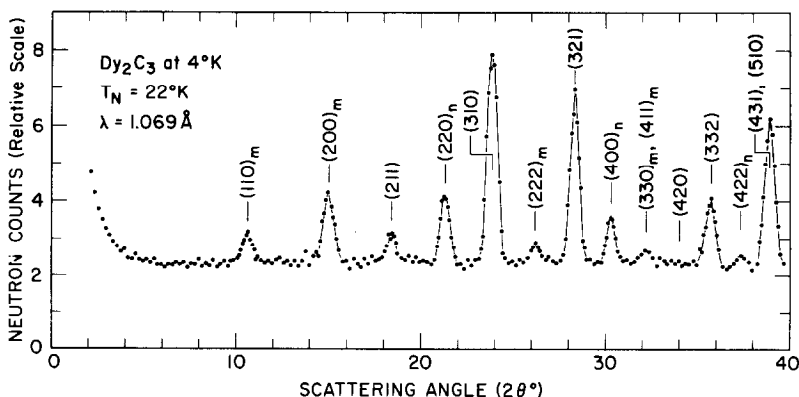


FIG. 3. Neutron diffraction pattern of the antiferromagnetically ordered  $\text{Dy}_2\text{C}_3$  at  $4^\circ\text{K}$ . The aluminum and impurity peaks have been subtracted out.

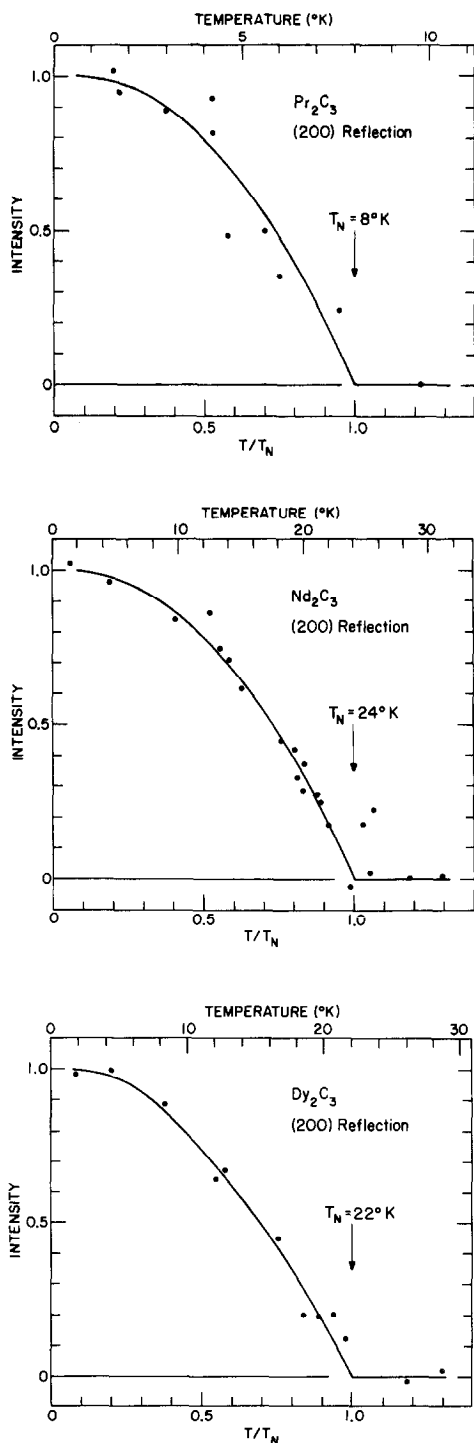


FIG. 4. The spontaneous magnetization in  $\text{Pr}_2\text{C}_3$ ,  $\text{Nd}_2\text{C}_3$ , and  $\text{Dy}_2\text{C}_3$ , represented by the integrated intensity of the magnetic (200) reflection.

$\text{Ho}_2\text{C}_3$  (11) is also approximated by the Brillouin function with  $J = 3$  ( $J = 8$  for  $\text{Ho}^{3+}$ ).

In  $(\text{RE})_2\text{C}_3$ , the RE atoms lie on four body diagonals. In the most probable uniaxial model for the  $\text{Tb}_2\text{C}_3$  magnetic structure (10), the RE atoms on two body diagonals exhibit an antiferromagnetic alignment, but those on the remaining two body diagonals show no ordering. Based on this model, the magnetic intensities of  $\text{Pr}_2\text{C}_3$ ,  $\text{Nd}_2\text{C}_3$ , and  $\text{Dy}_2\text{C}_3$  at temperatures near  $0^\circ\text{K}$  gave the ordered moments,  $gJ$  per RE = 1.3(2), 3.0(2), and 9.5-(3) Bohr magnetons ( $\mu_B$ ), where the free ion  $gJ$  values are 3.20, 3.27, and  $10.00 \mu_B$ , respectively. As found in  $\text{Tb}_2\text{C}_3$ , the most likely moment direction is parallel to either [011] or [111], and the deduced  $gJ$  values are practically independent of the moment direction. The uniaxial  $\text{Tb}_2\text{C}_3$  magnetic structure can be equivalently represented in a biaxial antiferromagnetic configuration in which all RE atoms have the ordered moment  $gJ = (gJ \text{ of the uniaxial model})^{1/2}$ . These magnetic structures of  $\text{Tb}_2\text{C}_3$  are rather unusual and hence were re-examined exhaustively. This effort, however, merely reconfirmed the previous results.

An external magnetic field of up to 21 kOe was applied to  $\text{Pr}_2\text{C}_3$ ,  $\text{Nd}_2\text{C}_3$ , and  $\text{Dy}_2\text{C}_3$  at 4.2 to  $1.6^\circ\text{K}$ . Both tightly and loosely packed powder samples were employed. The loose packing allows the orientation of the ferromagnetic particle in the direction of the external field. This field-induced orientation changes the neutron intensity of both the magnetic and nuclear reflections and can be effectively used to detect even feeble ferromagnetism (17). No field effect was observed in all but one of several  $\text{Nd}_2\text{C}_3$  samples examined. That particular  $\text{Nd}_2\text{C}_3$  sample displayed a small intensity enhancement on the ( $h00$ )-type reflections, inferring that the induced ferromagnetic moments are parallel to the cube axes. The field data, however, suffered from an irregular and irreversible hysteresis. Hence, the induced ferromagnetism should be parasitic, originating from various imperfections, multiform domain

boundaries, and the like. Consequently, it can be concluded that the intrinsic coupling in the  $\text{Tb}_2\text{C}_3$ -type magnetic alignment is hardly influenced by the field of up to 21 kOe.

## Discussion

The representative interatomic distances in  $(\text{RE})_2\text{C}_3$  are shown in Fig. 5. The C–C bond distances are all significantly longer than the acetylene C–C distance of 1.20 Å, suggesting that the C–C antibonding orbitals ( $\pi_g 2p$ ) participate in the valency bond hybridization with the RE orbitals (8, 14). In  $\text{Ce}_2\text{C}_3$ , an additional valency electron is available to the  $\pi_g 2p$  through  $\text{Ce}^{3+} \rightarrow \text{Ce}^{4+}$ , leading to the singularly longer C–C distance.

The bond distance between the RE atoms on the body diagonals,  $(\text{RE})_0-2(\text{RE})_2$  (8), is equal to  $3^{1/2}a/4$  ( $a$  = the lattice constant) and is about the same as the first-neighbor distance in the RE metal. Hence, the  $(\text{RE})_0-2(\text{RE})_2$  is likely to be of high  $s$ -character with a minor  $d$ -contribution, as realized in the RE metal. The trigonally arranged  $(\text{RE})_0-3(\text{RE})_1$  bonds are

considerably shorter than those in the RE metal and are probably of high  $d$ -character. These RE–RE bonds are closely conjugated to the RE–C bonds through the multiple-centered or asymmetric  $s-p-d$  hybridization. The  $RKKY$ , crystal field, and related magnetic interactions in  $(\text{RE})_2\text{C}_3$  should hence be considerably anisotropic, as demonstrated in the ordered moment configuration.

The instability of the  $\alpha$ - $(\text{RE})_2\text{C}_3$  crystal structure commences at  $\text{Ho}_2\text{C}_3$  and is progressively enhanced in the heavier RE. As shown in Fig. 2, this instability apparently occurs when the nonbonding distance,  $\text{C}_0 \cdots 4\text{C}_1$ , becomes shorter than the normal van der Waals C···C contact of 3.2 Å (18). The singularly unique magnetic structure of  $\text{Ho}_2\text{C}_3$  may be due to this lattice instability causing incongruous magnetoelastic interactions.

Carter *et al.* (19) have interpreted the  $\text{Pu}_2\text{C}_3$ -type structure without using the antibonding  $\pi_g 2p$  orbitals. In their approach, a 4 $f$  contribution of up to about 15% was considered in the orbital hybridization with specific reference to the  $\text{La}_2\text{C}_3$  interatomic distances. The extension of the theory to other  $(\text{RE})_2\text{C}_3$  and to their magnetic properties is of considerable interest.

The known Néel temperatures of  $\text{RE}_2\text{C}_3$  and  $\text{RE}\text{C}_2$  are compared in Fig. 6. In the light RE compounds, the crystal field effect is often predominantly large, as exemplified by the fact that Pr carbides have exceptionally low  $T_N$  and strongly suppressed ordered moments ( $1.14 \mu_B$  in  $\text{PrC}_2$ ). In the heavy RE, the exchange interaction and anisotropy energy become the major factors in the magnetization. We then set a molecular field equation,  $T_N = AX + B$ , where the DeGennes factor  $X = (g - 1)^2 J(J + 1)$  (20). The first term represents the  $RKKY$  bilinear scalar exchange interaction and the second term signifies mainly the anisotropy energy. For the heavy  $(\text{RE})_2\text{C}_3$ , a good fit is obtained with  $T_N = 2.38X + 7.15$ , indicating a relatively large anisotropy term. The heavy RE metals show an analogous

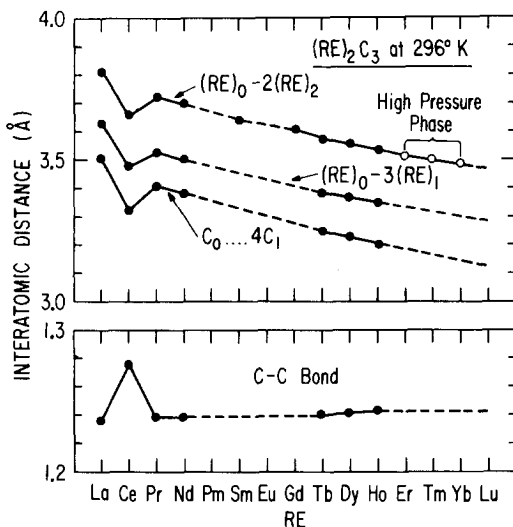


FIG. 5. The representative interatomic  $(\text{RE})_2\text{C}_3$  at 296°K. The filled and open circles denote the ambient and high-pressure phases, respectively. The  $(\text{RE})_0-2(\text{RE})_2$  distance is equal to  $3^{1/2}a/4$  and hence indicates the lattice constant variation also. For the atomic nomenclatures, see Ref. (8).

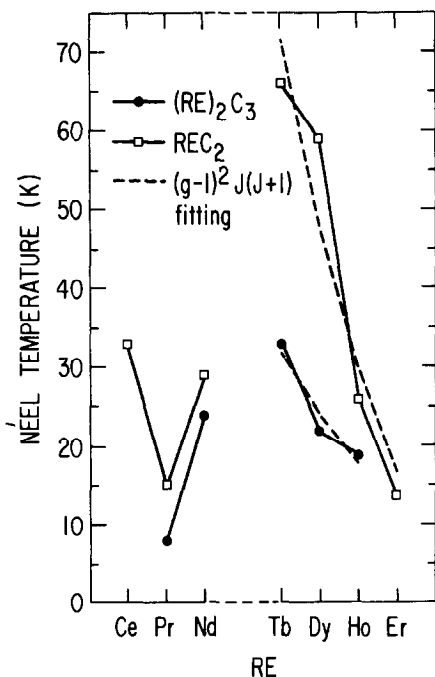


FIG. 6. The Néel temperatures of  $(RE)_2C_3$  and  $REC_2$ . For the heavy RE carbides, the DeGennes linear fit,  $T_N = AX + B$  where  $X = (g - 1)^2 J(J + 1)$ , is shown by broken lines.

relation,  $T_N$  (or  $T_C$ ) =  $16.2X + 50.6$ . For the heavy  $REC_2$ , a least-squares linear fit is  $T_N = 6.98X - 1.70$ , which gives rather poor agreement in Fig. 6. Moreover, the anisotropy term is negative. In  $REC_2$ , the anisotropic and/or higher-order exchange interaction may have to be considered and the crystal field effect is greatly different from that in  $(RE)_2C_3$  and the RE metals.

As regards other physical data, our temperature factor coefficients of  $(RE)_2C_3$  at 296°K give the Debye characteristic temperatures  $\theta_D$  (°K), 247(27), 344(29), 181(11), 181(11), 182(13), 177(12), and 176(9) for RE = La, Ce, Pr, Nd, Tb, Dy, and Ho, respectively. For RE = La, Ce, and Nd, Yupko *et al.* (21) have reported values of  $\theta_D = 189, 199$ , and 203°K, respectively, which are, except for  $Ce_2C_3$ , insignificantly different from our data. These  $\theta_D$  values of  $(RE)_2C_3$  are comparable to those of the rare earth metals (20) but are roughly 100° lower than those of  $REC_2$  (9).

Yupko *et al.* (21) have also measured the Hall coefficient and the electrical resistivity of  $La_2C_3$ ,  $Ce_2C_3$ ,  $Nd_2C_3$ , and  $Y_2C_3$ . The resulting electron carrier concentration data are, however, mutually inconsistent. Moreover, the electrical resistivity of  $La_2C_3$  at 20°C,  $340 \times 10^{-6} \Omega \text{ cm}$ , differs significantly from the value of  $144 \times 10^{-6} \Omega \text{ cm}$  reported elsewhere (1). These transport properties are particularly sensitive to impurities and refined measurements using the high-purity samples are highly desirable.

## References

1. F. H. SPEDDING, K. GSCHNEIDNER, JR., AND A. H. DAANE, *J. Amer. Chem. Soc.* **80**, 4499 (1958).
2. M. ATOJI, K. GSCHNEIDNER, JR., A. H. DAANE, R. E. RUNDLE, AND F. H. SPEDDING, *J. Amer. Chem. Soc.* **80**, 1804 (1958).
3. O. N. CARLSON AND W. M. PAULSON, *Trans. AIME* **242**, 846 (1968).
4. M. C. KRUPKA AND N. H. KRİKORIAN, in "Proceedings, 8th Rare Earth Research Conference," p. 582, Reno, Nev. (1970).
5. A. L. GIORGI, E. G. SZKLARZ, M. C. KRUPKA, AND N. H. KRİKORIAN, *J. Less-Common Metals* **17**, 121 (1969).
6. T. L. FRANCAVILLA AND F. L. CARTER, *Phys. Rev.* **B14**, 128 (1976).
7. M. C. KRUPKA, A. L. GIORGI, N. H. KRİKORIAN, AND E. G. SZKLARZ, *J. Less-Common Metals* **19**, 113 (1969).
8. M. ATOJI AND D. E. WILLIAMS, *J. Chem. Phys.* **35**, 1960 (1961).
9. M. ATOJI, *J. Chem. Phys.* **46**, 4148 (1967).
10. M. ATOJI, *J. Chem. Phys.* **54**, 3504 (1971).
11. M. ATOJI AND Y. TSUNODA, *J. Chem. Phys.* **54**, 3510 (1971).
12. M. ATOJI, *Nucl. Instr. Methods* **35**, 13 (1965); Argonne National Laboratory Rept. ANL-6920 (1964).
13. F. H. SPEDDING, K. GSCHNEIDNER, JR., AND A. H. DAANE, *Trans. AIME* **215**, 192 (1959).
14. M. ATOJI, *J. Chem. Phys.* **46**, 1891 (1967).
15. M. ATOJI, *J. Chem. Phys.* **48**, 3384 (1968).
16. N. F. M. HENRY AND K. LONSDALE (Eds.), "International Tables for X-ray Crystallography," Vol. I, Kynoch, Birmingham, England (1952).
17. M. ATOJI, I. ATOJI, C. DO-DINH, AND W. E. WALLACE, *J. Appl. Phys.* **44**, 5096 (1973).

18. M. ATOJI AND R. C. MEDRUD, *J. Chem. Phys.* **31**, 332 (1959).
19. F. L. CARTER, T. L. FRANCAVILLA, AND R. A. HEIN, in "Proceedings 11th Rare Earth Research Conference," Vol. I, p. 36, Traverse City, Mich. (1974).
20. R. J. ELLIOTT (Ed.), "Magnetic Properties of Rare Earth Metals," Plenum Press, New York (1972).
21. V. L. YUPKO, G. N. MAKARENKO, AND YU. B. PADERNO, in "Refractory Carbides" (G. V. Samsonov, Ed., N. B. Vaughan, Trans.), p. 251, Consultants Bureau, New York (1974).